EUROPEAN ORGANISATION FOR NUCLEAR RESEARCH

CERN-PPE/91-155
27 September 1991

A Measurement of Photon Radiation in Lepton Pair Events from Z^0 Decays

OPAL Collaboration

Abstract

We have measured the photon yield in lepton pair events recorded by the OPAL detector in a data sample corresponding to an integrated luminosity of 7.1 pb^{-1} at centre-of-mass energies between 88 GeV and 94 GeV. The results are compared to QED expectations for initial and final state photon radiation.

No anomalous photon yield has been found, and stringent limits on the branching ratio for exotic radiative three body Z^0 decays into a photon and a pair of leptons are obtained. We also place limits on possible Z^0 decays into a photon and a resonance X with subsequent decays of X into a pair of leptons.

Acollinear $\mu^+\mu^-$ events with missing momentum along the beam direction are identified as events with hard initial state photon radiation and used to measure an average cross section of 15 $\pm^{8}_{6}$ pb for e^+e^- annihilation into $\mu^+\mu^-$, in the so far untested range of centre-of-mass energies between 60 GeV and 84 GeV. This value is consistent with a cross section of 24 pb, expected from Z^0 and photon exchange.

Submitted to Physics Letters B

The OPAL Collaboration

P.D. Acton[25], G. Alexander[23], J. Allison[16], P.P. Allport[5], K.J. Anderson[9], S. Arcelli[2], P. Ashton[16], A. Astbury[a], D. Axen[b], G. Azuelos[18,c], G.A. Bahan[16], J.T.M. Baines[16], A.H. Ball[17], J. Banks[16], G.J. Barker[13], R.J. Barlow[16], J.R. Batley[5], G. Beaudoin[18], A. Beck[23], J. Becker[10], T. Behnke[27], K.W. Bell[20], G. Bella[23], P. Berlich[10], S. Bethke[11], O. Biebel[3], U. Binder[10], I.J. Bloodworth[1], P. Bock[11], B. Boden[3], H.M. Bosch[11], S. Bougerolle[b], B.B. Brabson[12], H. Breuker[8], R.M. Brown[20], R. Brun[8], A. Buijs[8], H.J. Burckhart[8], P. Capiluppi[2], R.K. Carnegie[6], A.A. Carter[13], J.R. Carter[5], C.Y. Chang[17], D.G. Charlton[8], P.E.L. Clarke[25], I. Cohen[23], W.J. Collins[5], J.E. Conboy[15], M. Cooper[22], M. Couch[1], M. Coupland[14], M. Cuffiani[2], S. Dado[22], G.M. Dallavalle[2], S. De Jong[8], P. Debu[21], L. Del Pozo[5], M.M. Deninno[2], A. Dieckmann[11], M. Dittmar[4], M.S. Dixit[7], E. Duchovni[26], G. Duckeck[11], I.P. Duerdoth[16], D.J.P. Dumas[6], G. Eckerlin[11], P.A. Elcombe[5], P.G. Estabrooks[6], E. Etzion[23], F. Fabbri[2], M. Fincke-Keeler[a], H.M. Fischer[3], D.G. Fong[17], C. Fukunaga[24], A. Gaidot[21], O. Ganel[26], J.W. Gary[4], J. Gascon[18], R.F. McGowan[16], N.I. Geddes[20], C. Geich-Gimbel[3], S.W. Gensler[9], F.X. Gentit[21], G. Giacomelli[2], V. Gibson[5], W.R. Gibson[13], J.D. Gillies[20], J. Goldberg[22], M.J. Goodrick[5], W. Gorn[4], C. Grandi[2], F.C. Grant[5], J. Hagemann[27], G.G. Hanson[12], M. Hansroul[8], C.K. Hargrove[7], P.F. Harrison[13], J. Hart[5], P.M. Hattersley[1], M. Hauschild[8], C.M. Hawkes[8], E. Heflin[4], R.J. Hemingway[6], R.D. Heuer[8], J.C. Hill[5], S.J. Hillier[1], D.A. Hinshaw[18], C. Ho[4], J.D. Hobbs[8], P.R. Hobson[25], D. Hochman[26], B. Holl[8], R.J. Homer[1], A.K. Honma[e], S.R. Hou[17], C.P. Howarth[15], R.E. Hughes-Jones[16], R. Humbert[10], P. Igo-Kemenes[11], H. Ihssen[11], D.C. Imrie[25], A.C. Janissen[6], A. Jawahery[17], P.W. Jeffreys[20], H. Jeremie[18], M. Jimack[2], M. Jobes[1], R.W.L. Jones[13], P. Jovanovic[1], D. Karlen[6], K. Kawagoe[24], T. Kawamoto[24], R.K. Keeler[a], R.G. Kellogg[17], B.W. Kennedy[15], C. Kleinwort[8], D.E. Klem[19], T. Kobayashi[24], T.P. Kokott[3], S. Komamiya[24], L. Köpke[8], F. Kral[8], R. Kowalewski[6], H. Kreutzmann[3], J. von Krogh[11], J. Kroll[9], M. Kuwano[24], P. Kyberd[13], G.D. Lafferty[16], F. Lamarche[18], W.J. Larson[4], J.G. Layter[4], P. Le Du[21], P. Leblanc[18], A.M. Lee[17], M.H. Lehto[15], D. Lellouch[26], P. Lennert[11], C. Leroy[18], L. Lessard[18], J. Letts[4], S. Levegrün[3], L. Levinson[26], S.L. Lloyd[13], F.K. Loebinger[16], J.M. Lorah[17], B. Lorazo[18], M.J. Losty[7], X.C. Lou[12], J. Ludwig[10], M. Mannelli[8], S. Marcellini[2], G. Maringer[3], A.J. Martin[13], J.P. Martin[18], T. Mashimo[24], P. Mättig[3], U. Maur[3], J. McKenna[a], T.J. McMahon[1], J.R. McNutt[25], F. Meijers[8], D. Menszner[11], F.S. Merritt[9], H. Mes[7], A. Michelini[8], R.P. Middleton[20], G. Mikenberg[26], J. Mildenberger[6], D.J. Miller[15], R. Mir[12], W. Mohr[10], C. Moisan[18], A. Montanari[2], T. Mori[24], M.W. Moss[16], T. Mouthuy[12], B. Nellen[3], H.H. Nguyen[9], M. Nozaki[24], S.W. O'Neale[8,d], B.P. O'Neill[4], F.G. Oakham[7], F. Odorici[2], M. Ogg[6], H.O. Ogren[12], H. Oh[4], C.J. Oram[e], M.J. Oreglia[9], S. Orito[24], J.P. Pansart[21], B. Panzer-Steindel[8], P. Paschievici[26], G.N. Patrick[20], S.J. Pawley[16], P. Pfister[10], J.E. Pilcher[9], J.L. Pinfold[26], D. Pitman[a], D.E. Plane[8], P. Poffenberger[a], B. Poli[2], A. Pouladdej[6], E. Prebys[8], T.W. Pritchard[13], H. Przysiezniak[18], G. Quast[27], M.W. Redmond[9], D.L. Rees[1], K. Riles[4], S.A. Robins[13], D. Robinson[8], A. Rollnik[3], J.M. Roney[9], E. Ros[8], S. Rossberg[10], A.M. Rossi[2,f], M. Rosvick[a], P. Routenburg[6], K. Runge[10], O. Runolfsson[8], D.R. Rust[12], S. Sanghera[6], M. Sasaki[24], A.D. Schaile[10], O. Schaile[10], W. Schappert[6], P. Scharff-Hansen[8], P. Schenk[a], H. von der Schmitt[11], S. Schreiber[3], J. Schwiering[3], W.G. Scott[20], M. Settles[12], B.C. Shen[4], P. Sherwood[15], R. Shypit[b], A. Simon[3], P. Singh[13], G.P. Siroli[2], A. Skuja[17], A.M. Smith[8], T.J. Smith[8], G.A. Snow[17], R. Sobie[g], R.W. Springer[17], M. Sproston[20], K. Stephens[16], H.E. Stier[10,†], R. Ströhmer[11], D. Strom[9], H. Takeda[24], T. Takeshita[24], P. Taras[18], S. Tarem[26], P. Teixeira-Dias[11], N.J. Thackray[1], T. Tsukamoto[24], M.F. Turner[5], G. Tysarczyk-Niemeyer[11], D. Van den plas[18], R. Van Kooten[8],

G.J. VanDalen[4], G. Vasseur[21], C.J. Virtue[19], A. Wagner[27], C. Wahl[10], J.P. Walker[1], C.P. Ward[5], D.R. Ward[5], P.M. Watkins[1], A.T. Watson[1], N.K. Watson[8], M. Weber[11], P. Weber[6], S. Weisz[8], P.S. Wells[8], N. Wermes[11], M. Weymann[8], M.A. Whalley[1], G.W. Wilson[21], J.A. Wilson[1], I. Wingerter[8], V-H. Winterer[10], N.C. Wood[16], S. Wotton[8], T.R. Wyatt[16], R. Yaari[26], Y. Yang[4,h], G. Yekutieli[26], M. Yurko[18], I. Zacharov[8], W. Zeuner[8], G.T. Zorn[17].

[1]School of Physics and Space Research, University of Birmingham, Birmingham, B15 2TT, UK
[2]Dipartimento di Fisica dell' Università di Bologna and INFN, Bologna, 40126, Italy
[3]Physikalisches Institut, Universität Bonn, D-5300 Bonn 1, FRG
[4]Department of Physics, University of California, Riverside, CA 92521 USA
[5]Cavendish Laboratory, Cambridge, CB3 0HE, UK
[6]Carleton University, Dept of Physics, Colonel By Drive, Ottawa, Ontario K1S 5B6, Canada
[7]Centre for Research in Particle Physics, Carleton University, Ottawa, Ontario K1S 5B6, Canada
[8]CERN, European Organisation for Particle Physics, 1211 Geneva 23, Switzerland
[9]Enrico Fermi Institute and Department of Physics, University of Chicago, Chicago Illinois 60637, USA
[10]Fakultät für Physik, Albert Ludwigs Universität, D-7800 Freiburg, FRG
[11]Physikalisches Institut, Universität Heidelberg, Heidelberg, FRG
[12]Indiana University, Dept of Physics, Swain Hall West 117, Bloomington, Indiana 47405, USA
[13]Queen Mary and Westfield College, University of London, London, E1 4NS, UK
[14]Birkbeck College, London, WC1E 7HV, UK
[15]University College London, London, WC1E 6BT, UK
[16]Department of Physics, Schuster Laboratory, The University, Manchester, M13 9PL, UK
[17]Department of Physics and Astronomy, University of Maryland, College Park, Maryland 20742, USA
[18]Laboratoire de Physique Nucléaire, Université de Montréal, Montréal, Quebec, H3C 3J7, Canada
[19]National Research Council of Canada, Herzberg Institute of Astrophysics, Ottawa, Ontario K1A 0R6, Canada
[20]Rutherford Appleton Laboratory, Chilton, Didcot, Oxfordshire, OX11 0QX, UK
[21]DPhPE, CEN Saclay, F-91191 Gif-sur-Yvette, France
[22]Department of Physics, Technion-Israel Institute of Technology, Haifa 32000, Israel
[23]Department of Physics and Astronomy, Tel Aviv University, Tel Aviv 69978, Israel
[24]International Centre for Elementary Particle Physics and Dept of Physics, University of Tokyo, Tokyo 113, and Kobe University, Kobe 657, Japan
[25]Brunel University, Uxbridge, Middlesex, UB8 3PH UK
[26]Nuclear Physics Department, Weizmann Institute of Science, Rehovot, 76100, Israel
[27]Universität Hamburg/DESY, II Inst. für Experimental Physik, 2000 Hamburg 52, FRG

[a]University of Victoria, Dept of Physics, P O Box 3055, Victoria BC V8W 3P6, Canada
[b]University of British Columbia, Dept of Physics, 6224 Agriculture Road, Vancouver BC V6T 1Z1, Canada
[c]Also at TRIUMF, Vancouver, Canada V6T 2A3
[d]On leave from Birmingham University, Birmingham B15 2TT, UK

[e]Univ of Victoria, Dept of Physics, P.O. Box 1700, Victoria BC V8W 2Y2, Canada and TRIUMF, Vancouver, Canada V6T 2A3
[f]Present address: Dipartimento di Fisica, Università della Calabria and INFN, 87036 Rende, Italy
[g]University of British Columbia, Dept of Physics, 6224 Agriculture Road, Vancouver BC V6T 2A6, Canada and IPP, McGill University, High Energy Physics Department, 3600 University Str, Montreal, Quebec H3A 2T8, Canada
[h]On leave from Research Institute for Computer Peripherals, Hangzhou, China
[†]deceased 25th March 1991

1 Introduction

Photon radiation from the initial and final state in e^+e^- collisions, as well as from particle decays is assumed to be a well-known and calculable QED process. Deviations in the photon yield of Z^0 decays into lepton pairs have been proposed in certain composite Z^0 models [1]. An anomalous photon yield in $\tau^+\tau^-(\gamma)$ events alone would indicate special electromagnetic properties of the τ lepton [2]. The rate of events with hard initial state radiation probes the e^+e^- annihilation cross section below the actual centre-of-mass energy and can thus be used to study e^+e^- annihilation processes for centre-of-mass energies between those of TRISTAN (60 GeV) and LEP.

In this paper we analyse radiative lepton pair events and search for anomalous photon sources in Z^0 decays into leptons. The photon yield is measured for the different types of lepton pair events and compared with predictions from the KORALZ[1] Monte Carlo program [3] as a function of angle and energy. If the only source of isolated photons were final state radiation, identical photon yields for $e^+e^-(\gamma)$, $\mu^+\mu^-(\gamma)$ and $\tau^+\tau^-(\gamma)$ events would be expected for photons above a certain minimal energy, for example 1 GeV. The sample of radiative events is used to search for three body Z^0 decays into a photon and a pair of leptons. We restrict the analysis largely to the barrel region to minimize t-channel contributions for the $e^+e^-(\gamma)$ final state, to reduce the confusion between initial and final state photon radiation, and to ensure that the detector has very good homogeneity and good resolution.

The paper is structured as follows:

Section 2: We give a brief description of the OPAL detector, the preselection of lepton pair events and the criteria used to identify the events as being $e^+e^-(\gamma)$, $\mu^+\mu^-(\gamma)$ or $\tau^+\tau^-(\gamma)$ events.

Section 3: We describe the measurement of the differential yield of photons as a function of angle and energy in $e^+e^-(\gamma)$, $\mu^+\mu^-(\gamma)$ and $\tau^+\tau^-(\gamma)$ events. From the comparison of the observed rate with QED expectations, limits are put on anomalous Z^0 photon couplings.

Section 4: A search for Z^0 decays into a photon and a narrow resonance X, with M_X between 60 GeV and 84 GeV, where X decays into any lepton pair is performed. A similar analysis has recently been performed by the L3 collaboration who searched for decays of X into e^+e^- and $\mu^+\mu^-$ [4].

Section 5: The analysis of acollinear $\mu^+\mu^-$ events with hard photons escaping along the beam direction (initial state radiation) and the measurement of the e^+e^- annihilation cross section into $\mu^+\mu^-$ for centre-of-mass energies between 60 GeV and 84 GeV.

[1]The KORALZ program is used with electroweak corrections, second order initial state radiation with exponentiation and first order final state radiation.

2 The experiment and the event selection

The data sample, which corresponds to an integrated luminosity of 7.1 pb^{-1}, was collected with the OPAL detector at LEP in 1989 and 1990. In a scan around the Z^0 resonance, 57% of the luminosity was collected with a centre-of-mass energy (E_{cm}) in the range $M_Z \pm 0.5$ GeV. For simplicity we shall refer to these data as the events at the peak.

2.1 The OPAL detector

This analysis is based on the central tracking chambers, the electromagnetic calorimeter and the muon detection system of the OPAL detector [5]. Charged tracking is provided by the central detector consisting of the vertex, jet, and z-chambers, inside a coil which provides a magnetic field of 0.435 T. The vertex chamber, containing 36 azimuthal[2] sectors of 12 axial sense wires and 36 sectors with six stereo sense wires, and the jet chamber, containing 24 sectors of 159 sense wires, are used to measure the momentum of charged particles. The z-chambers improve the momentum resolution by providing an accurate measurement of the polar angles of tracks.

The electromagnetic calorimeter contains a barrel ($|\cos\theta| < 0.82$) and two annular endcaps ($0.81 < |\cos\theta| < 0.98$). The barrel electromagnetic calorimeter consists of a cylindrical array of 9440 lead glass blocks of 24.5 radiation lengths (X_0) thickness that point approximately to the interaction region. The endcap electromagnetic calorimeter consists of 2264 lead glass blocks of 20 X_0 thickness, projecting along the beam axis. A cylindrical layer of 160 time-of-flight scintillation counters parallel to the beam axis is installed between the coil and the barrel electromagnetic calorimeter.

The barrel and endcap muon chambers, together with the hadron calorimeter, form the muon identification system, which covers polar angles in the range $|\cos\theta| < 0.98$. The barrel region of the muon chambers, covering the region $|\cos\theta| < 0.68$, consists of four layers of planar drift chambers, providing r, ϕ and z measurements. The endcap region, $0.60 < |\cos\theta| < 0.98$, is covered by four layers of limited streamer tubes, each layer measuring in the (x, z) and (y, z) planes. The hadron calorimeter, which consists of 9 (8) layers of streamer tubes interleaved with iron slabs of the magnet return yoke in the barrel (endcap), is read out via 4 mm wide strips and projective towers formed from 50×50 cm^2 pads. The strips provide measurements in the (r, ϕ) plane in the barrel, and in the (y,z) plane in the endcap.

The two forward detectors, each consisting of calorimeters, proportional tube chambers, drift chambers and scintillators, provide a luminosity measurement and complete the angular coverage of the electromagnetic calorimeter down to a polar angle of about 40 mrad.

To ensure good detector efficiency, we require the jet chamber of the central detector, the electromagnetic barrel and endcap calorimeter, the hadron calorimeter strips, the muon barrel detector, the forward detector, the track trigger and the barrel electromagnetic trigger to be fully operational.

[2]The coordinate system is defined with positive z along the outgoing e^- beam direction, θ and ϕ being the polar and azimuthal angles.

2.2 Quality requirements and topological definitions

For the following investigations we define good tracks, good electromagnetic clusters, muons, jets and the visible energy as follows:

- Good tracks must come from the interaction point. We require the distance of closest approach (d_0) of the track to the beam crossing point to be less than 5 cm projected perpendicular to the beam direction and less than 20 cm with respect to the beam direction (z_0) at the d_0 point. More than 30 wire hits (N_{hit}) of the jet chamber have to be associated with the track and the transverse momentum of the track with respect to the beam axis (p_t) has to be at least 150 MeV.

- Good electromagnetic clusters must have a raw energy deposit of more than 150 MeV. A cluster in the barrel region must consist of at least two blocks if its energy is larger than 1 GeV (the energy is corrected for the average energy loss of electrons in the coil). For the endcap lead glass calorimeter, we demand that clusters consist of at least three blocks.

- Muons are identified by matching central detector tracks with signals in the hadron calorimeter or the muon detector systems. We require that muons have a measured track momentum of more than 10% of the beam energy, $|\cos\theta|$ smaller than 0.75 and match in azimuth (within 50 mrad) with a reconstructed muon segment found independently in either the hadron calorimeter or the muon chambers. A muon segment must contain signals in at least 4 of 9 possible strip layers in the hadron calorimeter or in at least 3 of 4 possible layers in the muon chambers. To reduce hadronic backgrounds we use the information about the shower shape in the hadron calorimeter. We require a signature which is consistent with minimum ionizing particles (muons) by demanding that the total number of strip signals divided by the number of layers with signals be smaller than three.

- Jets are defined as collimated tracks and clusters and have to contain at least one track. We assign tracks to a jet if they are found within a cone around a jet axis. This assignment begins by choosing the track with the highest p_t. Taking the track direction as the starting direction of the jet, the other tracks are considered in descending order of p_t. If a track is found within 20° of the jet axis it is added to the jet, the jet momentum vector is recalculated and the search continues until all tracks have been considered. This process is repeated until all tracks have been assigned to jets. We then assign all electromagnetic clusters to jets if the clusters are found within the cone of 20° around the jet direction. The jet energy is the sum of all tracks and electromagnetic clusters associated with the jet. To avoid double counting for tracks with associated clusters, we use the larger energy of either the track or of the electromagnetic cluster. For tracks identified as muons, we use the sum of the track momenta and the calorimeter energy, but subtract the approximate average energy deposit of a muon in the lead glass calorimeter of 500 MeV.

- The total visible energy of an event, E_{vis}, is the sum of the jet energies plus the energy of all electromagnetic clusters not associated with a jet and with $|\cos\theta|$ less than 0.94. The electromagnetic energy of the event, E_{cal}, is the scalar sum of the energy of all the electromagnetic clusters with $|\cos\theta|$ less than 0.94.

2.3 Preselection of events and background rejection

The following cuts ensure that the events originate from an e^+e^- interaction and remove multi-hadronic events identified by the charged track multiplicity. We demand between 2 and 4 good tracks in the event; only 2% of the $\tau^+\tau^-$events, those where each τ decays into three or more charged particles. The background is further reduced by demanding that at least one track fulfills the requirement: $N_{hit} \geq 80$, $d_0 \leq 2$ cm, $p_t \geq 0.05 \times E_{beam}$ and $|\cos\theta| \leq 0.7$ (where E_{beam} is the beam energy). To remove cosmic ray events, we use the time-of-flight system and require that at least one time-of-flight counter, associated with a charged track, gives a time difference Δt of less than 5 ns between the measured time and the expected time for a particle coming from the interaction point. Further, the average ΔT of all Δt values from track-associated time-of-flight counters must satisfy $|\Delta T| \leq 5$ ns.

The jet algorithm is applied to the remaining 16327 events. We demand at least two reconstructed jets, one of them being within the barrel region, with $|\cos\theta_{jet}|$ less than 0.7, and the second one with $|\cos\theta_{jet}|$ less than 0.94. Events are rejected if there are more than two jets with an energy larger than 2% of the beam energy. We demand further that $x_{Evis} = E_{vis}/E_{cm}$ is larger than 0.05. The remaining 15866 events are dominantly lepton pairs coming from e^+e^- annihilation or two photon processes with small visible energies.

The following cuts are applied to reject two photon events:

- Tagged two photon events (events with a large energy deposit in the forward detector or the inner part of the endcap lead glass calorimeter) are rejected by requiring x_{fwd} to be smaller than 0.05, with $x_{fwd} = E_{fwd}/E_{cm}$. E_{fwd} is the sum of the energies deposited in the calorimeter of the forward detector and in the forward region of the endcap lead glass detector ($|\cos\theta|$ greater than 0.94).

- To distinguish τ-pair events with low visible energy from two photon events we also use the missing transverse momentum of the event due to the neutrinos in τ decays. For events which have a visible energy of less than 20% of E_{cm}, we require either the sum of the transverse jet momenta plus the isolated calorimeter clusters or the transverse vectorial energy sum of the electromagnetic calorimeter to be larger than 2 GeV.

- Finally we require that acollinear events, defined as events with an opening angle between the two jets of less than 160° , have at least one isolated electromagnetic cluster with $|\cos\theta|$ of less than 0.94 and with a cluster energy of more than 5% of E_{cm}. This cut rejects not only two photon events but also events with hard initial state radiation and undetected photons. These events will be discussed in section 5.

After these cuts 14443 events remain.

2.4 Lepton pair identification

To analyse the different types of radiative lepton pairs, we separate collinear and acollinear events. If the angle between the two jets is larger than 160° the events are called collinear,

otherwise they are called acollinear. Only in rare cases with very energetic isolated photons are the jets from Z^0 decays into lepton pairs acollinear. In order to identify the different types of lepton pairs we use the expected momentum and energy deposit in the detector:

- $e^+e^-(\gamma)$ events are characterised by the sum of the track momenta and the sum of the energy deposited in the electromagnetic calorimeter being close to the centre-of-mass energy.
- $\mu^+\mu^-(\gamma)$ events also have a sum of the track momenta close to the centre-of-mass energy and a very low associated electromagnetic energy deposit.
- $\tau^+\tau^-(\gamma)$ events are characterised by having both electromagnetic energy and track momentum sum smaller than the beam energy because of the undetected neutrinos.

We separate $e^+e^-(\gamma)$, $\mu^+\mu^-(\gamma)$ and $\tau^+\tau^-(\gamma)$ events in such a way that no significant bias in the yield of isolated photons is introduced. We use the scaled visible energy x_{Evis}, the scaled electromagnetic energy x_{Ecal}, and the number of jets containing tracks identified as muons. Figures 1a-d show a scatter plot of x_{Ecal} versus x_{Evis} for all events, and for the events with zero, one and two identified muons. The cuts applied below exclude some events which would not be unambiguously identified as a particular kind of lepton pair without introducing a bias against photon radiation (for example we require a positive identification of at least one muon and do not use $\mu^+\mu^-(\gamma)$ events that are identified only on the basis of their small energy deposit in the electromagnetic calorimeter and their high measured track momenta).

A small number of lepton pair events with an interaction of primary particles with atoms from the beam-pipe or the gas of the central detector are rejected on the basis of a high multiplicity of secondary particles. These secondary particles produced will not necessarily be associated with the event vertex and the reconstructed secondary tracks might not fulfill the d_0 requirement of the good track selection. As a result, the electromagnetic clusters associated with some of these secondary tracks would appear as isolated neutral clusters. These events are rejected by requiring that there are no more than eight reconstructed tracks with more than 30 associated hits and a transverse momentum of more than 150 MeV. Two $\mu^+\mu^-(\gamma)$ candidate events and 23 $\tau^+\tau^-(\gamma)$ candidate events, which fulfill all other requirements given below, are removed by this cut.

- To identify $e^+e^-(\gamma)$ events we require that both, x_{Evis} and x_{Ecal} are larger than 0.8. This requirement is fulfilled by 5618 events (3817 at the Z^0 peak).
- For $\mu^+\mu^-(\gamma)$ events at least one jet has to have a track identified as a muon. If both jets are identified as muons we demand x_{Evis} to be larger than 0.7. If only one jet is identified as a muon we demand x_{Evis} to be larger than 0.85. This requirement is fulfilled by 4483 events (3190 at the Z^0 peak).
- Among the remaining events we select $\tau^+\tau^-(\gamma)$ events with the following criteria:

  x_{Ecal} must be smaller than 0.75. If both jets are identified as muons, x_{Evis} must be smaller than 0.5. If no more than one jet is identified as a muon we use a combination of x_{Evis} and x_{Ecal} to separate $\tau^+\tau^-(\gamma)$ events from $\mu^+\mu^-(\gamma)$ events; we require that:

$$x_{Ecal} \geq 1.25 \times x_{Evis} - 0.75,$$

as indicated in figure 1b and 1c. A total of 3978 $\tau^+\tau^-(\gamma)$ events (2790 at the Z^0 peak) remains.

Table 1 contains the total number of events for each type of lepton pair on and off the Z^0 peak; the numbers for acollinear events are given in brackets.

2.5 Selection efficiency

We have studied the trigger efficiency using the independent trigger components comprising track-based triggers, electromagnetic calorimeter triggers and coincidences between trigger signals from the time-of-flight system and the muon chambers. A trigger efficiency greater than 99.9% for the selected different types of lepton pairs is found.

To determine the selection efficiency and backgrounds, we have applied the same criteria to Monte Carlo generated events [3], [6–9] with full detector simulation [10]. Reasonable agreement is observed between the relevant distributions in the data and the Monte Carlo. The errors on efficiencies and backgrounds, given below are statistical only.

- $e^+e^-(\gamma)$ events with both electrons within the geometrical acceptance are correctly identified with an efficiency of $(99 \pm 1)\%$. The background from $\tau^+\tau^-(\gamma)$ events is estimated to be $(0.25 \pm 0.05)\%$.
- $\mu^+\mu^-(\gamma)$ events are identified with an overall efficiency of $(61 \pm 1)\%$ (about 98% if both μ's are within the geometrical acceptance). The background from $\tau^+\tau^-(\gamma)$ events is $(1.0 \pm 0.1)\%$.
- $\tau^+\tau^-(\gamma)$ events are found with an efficiency of $(53 \pm 1)\%$ (about 87% if both τ's are within the geometrical acceptance). According to the Monte Carlo simulation, the background from misidentified $e^+e^-(\gamma)$ events and $\mu^+\mu^-(\gamma)$ events is $(0.4 \pm 0.1)\%$ and $(0.1 \pm 0.1)\%$ respectively. The background from misidentified hadronic- and two-photon events has been estimated from the Monte Carlo to be $(0.2 \pm 0.1)\%$ and $(0.4 \pm 0.2)\%$ respectively. Thus, a total background of $(1.1 \pm 0.3)\%$ is predicted for the $\tau^+\tau^-(\gamma)$ event sample.

A loss of radiative lepton pair events occurs because of the rejection of events with conversions of isolated photons, resulting in a third low multiplicity jet. We have studied the observed three jet events in detail and found 12 $e^+e^-(\gamma)$ and eight $\mu^+\mu^-(\gamma)$ events with all three jets within the barrel region which fulfill the above criteria on the number of muons and the visible event energy. These numbers are in very good agreement with an expectation of 8.2 ± 2.4 and 8.6 ± 1.9 events from the $e^+e^-(\gamma)$ and $\mu^+\mu^-(\gamma)$ Monte Carlo simulation respectively. This result is also in good agreement with a recent study of photon conversions in $e^+e^- \rightarrow \gamma\gamma$ events, which has determined a conversion probability in the central detector of $(5.7 \pm 2.2)\%$ in the

data and a value of (5.9 ± 0.7) % in the Monte Carlo [11]. We follow the procedure applied there and correct in the following all our photon rates by 6% with an uncertainty of 2%.

We conclude that, compared to the statistical accuracy of the measurements which is about 10% or more, uncertainties in the efficiencies and the remaining background can be neglected. In addition, since no significant bias to the photon yield relative to the number of accepted lepton pairs is introduced by the event selection, the analysis is insensitive to small imperfections in the Monte Carlo simulation.

3 The energy spectrum of photons in lepton pair events and their angular separation

We now describe the measurement of the angular separation between charged leptons and photon candidates with energies larger than 2% of the beam energy. First, we study collinear photon radiation and then the isolated photon yield. The isolated photon yield is compared between the different types of lepton pairs and with Monte Carlo expectations for photon radiation. We use this measurement to search for possible three body Z^0 decays into a photon and a lepton pair. For this search the data at the Z^0 peak are used, in order to minimize the contributions from initial state radiation. We require that the average value $|\cos\theta_{jet}|$ of both jets is smaller than 0.7. We define the scaled photon energy x_γ $(= E_\gamma/E_{beam})$ and $\alpha_{\ell\gamma}$, the angle between the photon and the closest lepton (jet). The number of collinear events for each lepton pair channel on and off the peak is given in Table 2.

The collinear radiation yield (e.g. $\alpha_{\ell\gamma}$ smaller than 100 mrad) is expected to have a significant dependence on the lepton mass (m_ℓ). The rate of collinear photons should be proportional to $\ln(s/m_\ell^2)$ where $s = E_{cm}^2$ [12]. An additional small enhancement in $\tau^+\tau^-(\gamma)$ events is expected from photon radiation in the τ decay which depends on the specific decay mode. With the current statistics we cannot, however, observe this mass dependence, but can check how well the collinear photon rate for $e^+e^- \to \mu^+\mu^-\gamma$ is described by the KORALZ Monte Carlo.

For larger $\alpha_{\ell\gamma}$ angles and x_γ larger than 0.02 the yield of photons is expected to be independent of the specific type of lepton pair.

3.1 Collinear photon radiation

For this analysis we compare the electromagnetic energy associated with the jets (within a cone of 20° around the jet direction) with the KORALZ Monte Carlo. For consistency with the analysis of isolated photons, we use here only the data at the peak. Only the muons can be used reliably in the study of the collinear photon yield, since they are usually minimum ionising in the electromagnetic calorimeter, allowing their energy deposit to be subtracted reliably on an average basis.

An indirect measurement for $e^+e^-(\gamma)$ events has been investigated by using the difference

between the beam energy and the measured track momenta for the photon energy. However, in a Monte Carlo study, we found that about 80% of these indirectly determined photons with x_γ above 0.3 are secondary photons produced by electron bremsstrahlung in the central detector material. Therefore no statement about the primary collinear radiation can be made for $e^+e^-(\gamma)$ events.

In the $\mu^+\mu^-(\gamma)$ events, the energy of collinear photons is defined as the total calorimeter energy associated with the jet, where 500 MeV, roughly equivalent to the energy deposit of muons, has been subtracted. Out of the collinear 3124 $\mu^+\mu^-(\gamma)$ events at the peak, 476 events have at least one photon candidate with x_γ above 0.02 (319 events with x_γ above 0.05). From KORALZ $\mu^+\mu^-(\gamma)$ events passed through the full detector simulation, the efficiency for x_γ larger than 0.05 is found to be 100% within the errors. According to the full detector simulation where electromagnetic interactions of muons are simulated, 50% of the photon candidates with x_γ between 0.02 and 0.05 are due to background from μ bremsstrahlung within the calorimeter itself; for x_γ between 0.05 and 0.1, this background is reduced to 20% and to about 5% for higher photon energies. Figure 2 shows the distribution of x_γ for collinear photons relative to the number of collinear $\mu^+\mu^-(\gamma)$ events, after the background subtraction and the efficiency correction. To take uncertainties of the detector simulation into account, a 20% systematic error on the background from muon interactions is included in the calculated errors. Agreement is observed between the data and the expectation from the KORALZ Monte Carlo. The curves in figure 2 and in the following figures are smoothed Monte Carlo distributions from about a factor of four more statistics compared to the data.

For $\tau^+\tau^-(\gamma)$ events we have investigated the collinear photon yield in the events where we can identify a clean muon from a τ decay. Photons are identified using the same method as for $\mu^+\mu^-(\gamma)$ events. Even though strong criteria based on the shower shape in the hadron calorimeter are used to identify clean τ decays into μ's, the background contamination from hadronic τ decays for the obtained photon candidates is still about 40%. Therefore, with the current statistics no clear statement about the rate of collinear photons in $\tau^+\tau^-(\gamma)$ events is yet possible.

3.2 The angular distribution of isolated photons with respect to the lepton

From the above measurement of collinear photons we know that the collinear radiation in $e^+e^- \to \mu^+\mu^-(\gamma)$ events is well described within the current statistical precision by the KORALZ program with first order final state radiation. Deviations in the energy or in the angular distributions of isolated photons in the lepton pair events from the KORALZ predictions might be a sign for new photon sources.

We consider electromagnetic clusters as photons if $|\cos\theta|$ is smaller than 0.7, the scaled energy x_γ is larger than 0.02, and there is no associated track. We count isolated photons in $e^+e^-(\gamma)$ and $\mu^+\mu^-(\gamma)$ events if the clusters are separated by more than 200 mrad from the tracks; for $\tau^+\tau^-(\gamma)$ events this separation angle is increased to more than 300 mrad to eliminate the background from π^0's in τ decays.

From a Monte Carlo study we find that the only significant loss in efficiency occurs because

of photon conversions inside the central detector, giving an estimated inefficiency of $(6 \pm 2)\%$ as described in section 2.4. Figures 3a–c show the differential photon yield per collinear lepton pair event as a function of the separation angle $\alpha_{\ell\gamma}$ for bands of x_γ between 0.02–0.10, 0.10–0.30 and 0.30–1.0. Within the given statistical accuracy, the same photon yield for the different types of lepton pairs is observed, in good agreement with the expectations of QED. The curves in figures 3a–c are the Monte Carlo expectations for $\mu^+\mu^-(\gamma)$ events (with a factor of four higher statistics than the data) where the same cuts are applied.

Figure 3d shows the energy spectrum of the isolated photons for angles $\alpha_{\ell\gamma}$ larger than 0.5 radians. These events can be used to set limits on possible three body Z^0 decays. The observed energy distribution is in good agreement with the expectations from final state radiation, giving no evidence for anomalous three body Z^0 decays. The number of such isolated photons with x_γ greater than 0.02 is given in Table 2 for each lepton pair channel along with the expected number of photons from the KORALZ Monte Carlo events, after the full detector simulation.

To determine 95% confidence level upper limits on a possible excess of events containing photons, $N_{\ell\ell\gamma}^{extra}$ we increase the number of isolated photons by two standard deviations and subtract the expected number of background events from QED radiation. For this background estimate we use the KORALZ Monte Carlo expectations for $\mu^+\mu^-(\gamma)$ events for the three types of $\ell^+\ell^-\gamma$ events. This is also justified for $e^+e^-(\gamma)$ events at the peak, where about 85% of the events come from Z^0 decays within the given angular cuts. KORALZ provides a better description of the isolated photon yield for $e^+e^-(\gamma)$ events than the existing first order $e^+e^-(\gamma)$ Monte Carlo [6], which predicts about 30% more photons in $e^+e^-(\gamma)$ events.

To transform this limit on $N_{\ell\ell\gamma}^{extra}$ into a branching ratio limit on Z^0 decay into a photon and a pair of leptons, we have to correct for efficiencies and normalize to the total number of Z^0 decays used. In the absence of any well defined theoretical prediction for these decays, we simulate isotropic three body Z^0 decays using the Lund Monte Carlo framework [7]. We choose to normalize to the number, $N_{\ell^+\ell^-}$, of collinear lepton pair events for each channel, using $BR(Z^0 \to \ell^+\ell^-) = 0.0333 \pm 0.0003$, which is the leptonic branching ratio of the Z^0 measured by OPAL [13], and $\varepsilon_{\rm geom} = (64 \pm 2)\%$, which is the ratio of the geometrical efficiency for three body Z^0 decays to the geometrical efficiency for collinear $\ell^+\ell^-(\gamma)$ events in the barrel region.

Limits for the Z^0 branching ratio for three body decays are then obtained separately for $e^+e^-\gamma$, $\mu^+\mu^-\gamma$ and $\tau^+\tau^-\gamma$ using the relation

$$BR(Z^0 \to \ell^+\ell^-\gamma) < \frac{N_{\ell\ell\gamma}^{extra} \cdot BR(Z^0 \to \ell^+\ell^-)}{\varepsilon_{geom} \cdot \varepsilon_\gamma \cdot N_{\ell^+\ell^-}}, \qquad (1)$$

$\varepsilon_\gamma = 0.94 \pm 0.02$ is the efficiency to identify an isolated photon.

For the three body limit of $e^+e^-\gamma$ events we cannot obtain the number of Z^0 decays directly from the ratio of the leptonic branching ratio and the observed number of $e^+e^-(\gamma)$ events because of the t-channel contribution. Instead, since nearly all $e^+e^-(\gamma)$ events within the geometrical acceptance are identified, we use the ratio $N_{\mu^+\mu^-}/BR(Z^0 \to \ell^+\ell^-(\gamma))$ to represent the total number of Z^0 decays. No systematic error is assigned to this method.

We add all systematic uncertainties in quadrature and increase our limits by one standard deviation. The overall systematic error is estimated to be 6%, assuming uncertainties of 5%

from the predicted number of QED background events, 1% from the uncertainty of the leptonic Z^0 branching ratio and 3% from the efficiency corrections including the photon conversion corrections. The obtained 95% confidence level limits for such anomalous three body Z^0 decays are summarised in Table 2. These limits are about a factor of 60 smaller than our measured leptonic partial width of the Z^0 .

4 Search for Z^0 decays into a photon and a narrow resonance X

The search for a narrow resonance is not very sensitive to the detailed understanding of initial and final state radiation. We therefore use all lepton pairs from the data on and off the peak and enlarge the acceptance for energetic photons, as compared to the analysis described in section 3, by including the endcap region. The following criteria are used:

1. We require events with two jets and at least one isolated electromagnetic cluster, which is assumed to be the photon. The scaled photon energy x_γ has to be larger than 0.1 and $|\cos\theta|$ must be smaller than 0.94. To obtain good energy resolution, photons with $|\cos\theta|$ between 0.75 and 0.82, where additional passive material degrades the energy resolution, are not considered for this analysis.
2. One of the jets and either the photon or the second jet has to be found within $|\cos\theta_{jet}| < 0.7$.

A total of 404 events fulfill the above conditions, six of which have two isolated energetic photons. The different types of lepton pairs are identified, using the selection criteria based on energy and momentum described in section 2.

The recoil mass spectra between 50 GeV and 90 GeV, calculated from the photon energy, for $e^+e^-(\gamma)$, $\mu^+\mu^-(\gamma)$, $\tau^+\tau^-(\gamma)$ and for the undifferentiated lepton pairs, do not show any resonance-like structure and are in good agreement with the Monte Carlo expectation. The accuracy of the photon energy measurement results in a resolution, at one standard deviation, of 0.5 GeV for a recoil mass of $M_X = 80$ GeV and increases to 1.5 GeV at $M_X = 60$ GeV.

To calculate 95% confidence level upper limits on the branching fraction of the Z^0 decay into a photon and a hypothetical resonance X, $BR(Z^0 \to X\gamma)$, we follow the procedure of section 3.2 and use relation 1. The maximum number of events for a given mass interval is obtained by increasing the number of observed events by two standard deviations and subtracting the background expected from the Monte Carlo. The mass resolution is taken into account by choosing 2 GeV bins for a recoil mass below 74 GeV, and 1 GeV bins for a recoil mass above 74 GeV.

The upper limit on the number of excess events is corrected for efficiency by a Monte Carlo simulation of isotropic Z^0 decays into $X\gamma$ with the subsequent decays of the X into a pair of leptons, using the Lund Monte Carlo framework [7]. The efficiency to find such Z^0 decays is $(61 \pm 2)\%$ for both $e^+e^-\gamma$ and $\mu^+\mu^-\gamma$ events. For $\tau^+\tau^-\gamma$ events the efficiency is lower $(53 \pm 2\%)$. Events with photon conversions before the coil are rejected giving an inefficiency of $(6 \pm 2)\%$.

The total number of Z^0 decays is obtained from the ratio of the number of observed $\mu^+\mu^-(\gamma)$ events divided by the efficiency to identify $\mu^+\mu^-(\gamma)$ events (see section 2.5) and our measured leptonic branching ratio [13]. Systematic uncertainties are taken into account by increasing the limits as in section 3.2 by a factor of 1.06.

The limits on the branching ratios for $Z^0 \rightarrow X\gamma$ with subsequent decays of X into e^+e^-, $\mu^+\mu^-$, $\tau^+\tau^-$ and $\ell^+\ell^-$ are shown in figures 4a-d; some values are also given in Table 3.

5 Analysis of acollinear dilepton events without observed photons

In this section we analyse the events which have a large acollinearity angle between the two jets and no detected isolated photon. Exotic events with weakly interacting neutral particles might be identified by such a signature. Lepton pair events with energetic but undetected photons are conventional sources for these events. In the case of nearly complete electromagnetic calorimeter coverage, the photon must either be reconstructed or should escape along the beam pipe. In the latter case the photon does not carry any significant transverse momentum and the two leptons have to be coplanar with the beam direction.

The lepton pair events with missing photons along the beam direction are predominantly events with hard initial state radiation. The rate for these events is proportional to the dilepton cross section well below the actual centre-of-mass energy. These events may therefore be used to measure the dilepton cross section between the TRISTAN energies (60 GeV) and the LEP energies.

5.1 Acoplanar events

First we search for acoplanar dilepton events by studying the collinearity of the two jet momenta projected onto the plane orthogonal to the beam direction. We define the acoplanarity angle $\phi_{\rm acop}$ as the angle between these projected momenta. This analysis is essentially the same as the one used in an early publication on a search for exotic processes [14] but is based on a 14 times larger sample. We select all events which have two charged jets (leptons), at least one of which has to be found within $|\cos\theta|$ less than 0.7. The energy of each jet must exceed 6% of the beam energy and the missing transverse momentum of the two jets should be larger than 6% of the beam energy. The events with isolated photons are removed by requiring that the energy sum of all electromagnetic clusters (including the clusters detected in the forward detector) not associated with the two jets has to be smaller than 2% of the centre-of-mass energy. No event with an acoplanarity angle of more than 20° is found, showing that except for the beam pipe, there is no significant gap in the acceptance, and that there is no indication of events with the recoil of an exotic weakly interacting particle.

5.2 Acollinear events

We now analyse the acollinear events that are coplanar with the beam and have no isolated neutral clusters in the electromagnetic calorimeter. To select these events we start from the preselected low multiplicity sample described in section 2 and require that:

1. there should be exactly two charged jets each with a momentum of more than 2 GeV, both of them having $|\cos\theta|$ less than 0.7;
2. the electromagnetic energy outside the two jets and well inside of the endcap lead-glass calorimeter ($|\cos\theta|$ smaller than 0.96) be smaller than 2% of the centre-of-mass energy;
3. the angle $\phi_{\rm acop}$ between the two jets, measured in the transverse plane, satisfy $\cos\phi_{\rm acop}$ less than –0.94;
4. the opening angle $\theta_{\rm 3D}$ between the two jets, calculated from the tracks and from the electromagnetic clusters separately, should both satisfy $\cos\theta_{\rm 3D} > -0.98$.

With these criteria 271 events with large missing energy along the beam direction are selected.

We are mainly interested in studying the e^+e^- annihilation cross section into leptons at energies below the Z^0 energy. The $\mu^+\mu^-(\gamma)$ channel gives the clearest signal. The $e^+e^-(\gamma)$ events are dominated by t-channel photon exchange but can be used to cross check the calculated missing photon energy. The $\tau^+\tau^-(\gamma)$ events with hard initial state radiation are more difficult to identify because of the large missing energy and momentum of the neutrinos and are not considered further.

If the unseen photon direction is along the beam axis we can use the constraints from the three body kinematics. The photon energy E_γ^{angle} can be determined from the measured jet angles and from the centre-of-mass energy with good accuracy for e^+e^- and $\mu^+\mu^-$ events. The e^+e^- and $\mu^+\mu^-$ events with hard initial state radiation along the beam can then be distinguished from two photon and $\tau^+\tau^-$ events by requiring that the total energy of the event E_{tot}, taken as the sum of the measured energy of the two jets plus the calculated energy of the missing photon, is close to the centre-of-mass energy.

For the selection of such $e^+e^-(\gamma)$ events we require the energy sum in the electromagnetic calorimeter plus E_γ^{angle} to be larger than 80% of the centre-of-mass energy. This cut is satisfied by 67 events. The calculated e^+e^- mass spectrum does not show any structure. As most of these events are expected to be produced by t-channel exchange we use them to check how well the photon energy can be calculated from the angles. The photon energy $E_\gamma^{energy} = (E_{cm} - E_{calorimeter})$ can also be calculated, with small errors in $e^+e^-\gamma$ events. From the difference $(E_\gamma^{angle} - E_\gamma^{energy})$ we determine a resolution of one standard deviation for E_γ^{angle} of 1.7 GeV at an average photon energy of 17 GeV.

The accuracy of the energy determination from the angles has also been studied using the $\ell^+\ell^-\gamma$ events with isolated photons selected as described in section 3. From the $e^+e^-\gamma$ and $\mu^+\mu^-\gamma$ events with energetic detected photons with energies above 5 GeV and with an average energy of 27 GeV, we find a resolution of 1.4 GeV for E_γ^{angle} from the comparison of the measured and the calculated photons energies.

5.3 Acollinear $\mu^+\mu^-$ γ events

For the selection of the acollinear $\mu^+\mu^-$ events with hard photon radiation along the beam axis we require that the total electromagnetic calorimeter energy be smaller than 2% of the centre-of-mass energy. The cut is satisfied by 95 events. The total scaled energy distribution of these events is shown in figure 5a together with the background expectation from two photon Monte Carlo events of the type $e^+e^- \rightarrow e^+e^-\mu^+\mu^-$ [9]. Most of the obtained events have a very low visible energy and are consistent with the Monte Carlo expectations for two photon events.

We identify events as being $\mu^+\mu^-\gamma$ events, with a γ emitted along the beam direction, if E_{tot} is larger than 80% of the centre-of-mass energy. Seven events in the data, well separated from the others, have total energies close to the centre of mass energy.

From a sample of two photon Monte Carlo events, corresponding to twice the accumulated integrated luminosity, we find one event which satisfies the above cut. From a high statistics generator level study of two photon events we estimate a contribution of 0.07 ± 0.01 such events in the data.

Five of the seven identified $\mu^+\mu^-$ events have an effective dilepton centre-of-mass energy between 60 GeV and 84 GeV. To determine a cross section for e^+e^- annihilation at these effective centre-of-mass energies we generated events with the KORALZ Monte Carlo program with initial and final state photon radiation. To obtain high statistics, no detector simulation was applied for this study and events were generated at the seven different centre-of-mass energies where data were recorded. To determine the efficiency to identify correctly the events with hard initial state radiation we apply the same geometrical and kinematical cuts as for the data. If both muons are within the geometrical acceptance, 92% of the events with hard initial state radiation are selected. The loss arises from events with E_{cal}/E_{cm} larger than 0.02 due to the presence of additional photons. This efficiency is in good agreement with an estimate using the full detector simulation. Conservatively we assign a systematic error of 10% for the efficiency and 1% for the possible two photon background.

For the integrated luminosity corresponding to the data sample we expect to find 8 ± 1 $\mu^+\mu^-\gamma$ events for effective dilepton centre-of-mass energies $\sqrt{s'}$ between 60 GeV and 84 GeV. This number can be compared to the five observed events in this energy range. Table 4 shows the number of events found and expected for different $\sqrt{s'}$ intervals, the input Born cross section and our cross section measurement.

Our results for the $\mu^+\mu^-$ Born cross section at the average centre-of-mass energy of 75 GeV is shown in figure 5b, together with previously measured values at lower energies [15] and our recent measurements of the total $\mu^+\mu^-(\gamma)$ cross section around the Z^0 peak [13]. The curve shows the Standard Model Born cross section.

6 Summary

We have measured the photon yield in lepton pair events as a function of the energy and of the isolation angle. We find the same photon yield in $e^+e^-(\gamma)$, $\mu^+\mu^-(\gamma)$ and $\tau^+\tau^-(\gamma)$ events at the

Z^0 peak for isolated photons with energies of more than 2% of the beam energy. This photon yield is in good agreement with expectations from QED final state radiation. No indication of anomalous photon production is found. We obtain the following branching ratio limits at 95% confidence limit for exotic three body Z^0 decays:

$$BR(Z^0 \rightarrow e^+e^-\gamma) < 5.2 \times 10^{-4}$$
$$BR(Z^0 \rightarrow \mu^+\mu^-\gamma) < 5.6 \times 10^{-4}$$
$$BR(Z^0 \rightarrow \tau^+\tau^-\gamma) < 7.3 \times 10^{-4}$$

We have searched for peaks in the recoil mass spectrum calculated from the photon energy. The branching ratio $BR(Z^0 \rightarrow X\gamma) \times BR(X \rightarrow \ell^+\ell^-)$ must be smaller than 1.1×10^{-4} at the 95% confidence level for any possible resonance X with a mass between 60 GeV and 82 GeV.

A sample of acollinear $\mu^+\mu^-$ pair events with hard initial state photon radiation close to the beam direction has been identified. These events are used to measure the cross section for e^+e^- annihilation into $\mu^+\mu^-(\gamma)$ in the so far untested centre-of-mass energy range between the directly accessible TRISTAN range and the Z^0 peak. We measure a cross section of $15\pm^{8}_{6}$ pb at an average centre-of-mass energy of 75 GeV, consistent with the Standard Model prediction of 24 pb.

Acknowledgements

We thank Z. Was for many interesting discussions and suggestions concerning the analysis of radiative lepton pair events. We also profited from discussions with F. Renard about composite models. We also thank J. Raab who contributed to this analysis at an early phase.

It is a pleasure to thank the SL Division for the efficient operation of the LEP accelerator, the precise information on the absolute energy, and their continuing close cooperation with our experimental group. In addition to the support staff at our own institutions we are pleased to acknowledge the
Department of Energy, USA,
National Science Foundation, USA,
Science and Engineering Research Council, UK,
Natural Sciences and Engineering Research Council,Canada,
Israeli Ministry of Science,
Minerva Gesellschaft,
Japanese Ministry of Education, Science and Culture (the Monbusho) and a grant under the Monbusho International Science Research Program,
American Israeli Bi-national Science Foundation,
Direction des Sciences de la Matière du Commissariat à l'Energie Atomique, France,
Bundesministerium für Forschung und Technologie, FRG,
A.P. Sloan Foundation and Junta Nacional de Investigação Científica e Tecnológica, Portugal.

References

[1] See for example: Z Physics at LEP 1, eds. G. Altarelli, R. Kleiss and C. Verzegnassi (1989) Vol. 2 page 185-211 and S. Moubarik, Thèse de Doctorat - Université de Provence (France) (1990). See also W. Bernreuther, U. Löw, J.P. Ma and O. Nachtmann, Z. Phys. **C43** (1989) 117.

[2] J.A. Grifols and A. Mendez, UAB-FT-254 (November 90).

[3] S. Jadach, B.F.L. Ward, Z. Was, R.G.S. Stuart, and W. Hollik, KORALZ, to be published in Comp. Phys. Comm., CERN-TH-5994-91.

[4] L3 Collaboration, B. Adeva et al., Phys. Lett. **B262** (1991) 155-162.

[5] OPAL Collaboration, M. Ahmet et al., Nucl. Inst. Meth. **A305** (1991) 275-319.

[6] F. A. Berends, R. Kleiss and W. Hollik, DESY 87-094.

[7] T. Sjöstrand, Comp. Phys. Comm. **39** (1986) 347.

[8] F.A. Berends, P.H. Daverveldt and R. Kleiss, Comp. Phys. Comm. **40** (1986) 271, 285, 309.

[9] R. Bhattacharya, J. Smith and G. Grammer, Phys. Rev. **D15** (1977) 3267;
J. Smith, J.A.M. Vermaseren and G. Grammer, Phys. Rev. **D15** (1977) 3280.

[10] J. Allison et al., Comp. Phys. Comm. **47** (1987) 55;
D. Ward, Proceedings of the MC'91 Workshop, NIKHEF, Amsterdam, 1991.

[11] OPAL Collaboration, M. Z. Akrawy et al., Zeit. Phys. **C50** (1991) 373-384.

[12] Private communication Z. Was.

[13] OPAL Collaboration, G. Alexander at al., CERN-PPE/91-67.

[14] OPAL Collaboration, M.Z. Akrawy et al., Phys. Lett. **B240** (1990) 261.

[15] A. Maki, Results from TRISTAN, Proc. 14. Int. Symp. on Lepton and Photon Interactions, Stanford, 1989, ed. M. Riordan, (World Scientific, Singapore, 1990), p. 203.

	$e^+e^-(\gamma)$	$\mu^+\mu^-(\gamma)$	$\tau^+\tau^-(\gamma)$
on peak	3778 (39)	3157 (33)	2764 (26)
off peak	1766 (35)	1282 (11)	1168 (20)

Table 1: The number of identified collinear lepton pair events on and off the Z^0 peak. The numbers in brackets give the number of acollinear lepton pairs.

Data on peak			
$Z \to \ell^+\ell^-\gamma$	$e^+e^-(\gamma)$	$\mu^+\mu^-(\gamma)$	$\tau^+\tau^-(\gamma)$
$N^{coll}_{\ell+\ell-}$	3698	3124	2661
N_γ (Data)	123	108	103
N_γ (MC)	117 ± 6	99 ± 5	90 ± 3
$N_\gamma/N^{coll}_{\ell+\ell-}$ (Data) ($\times 10^{-2}$)	3.3 ± 0.3	3.5 ± 0.3	3.9 ± 0.4
$N_\gamma/N^{coll}_{\ell+\ell-}$ (MC) ($\times 10^{-2}$)	3.2 ± 0.2	3.2 ± 0.2	3.4 ± 0.1
Data off peak			
$Z \to \ell^+\ell^-\gamma$	$e^+e^-(\gamma)$	$\mu^+\mu^-(\gamma)$	$\tau^+\tau^-(\gamma)$
$N^{coll}_{\ell+\ell-}$	1701	1277	1122
N_γ	79	42	45
$N_\gamma/N^{coll}_{\ell+\ell-}$ ($\times 10^{-2}$)	4.6 ± 0.5	3.3 ± 0.5	4.0 ± 0.6
Limits for $Z \to \ell^+\ell^-\gamma$			
limit N^{extra}_γ (95% c.l.)	28	30	33
$BR(Z \to \ell^+\ell^-\gamma)$ limit	5.2×10^{-4}	5.6×10^{-4}	7.3×10^{-4}

Table 2: The numbers of collinear lepton pair events and the number of events with isolated photons and x_γ above 0.02 in the data on and off the Z^0 peak, the Monte Carlo expectation on the Z^0 peak and the ratio of events with photons to the number of collinear lepton pair events. The calculated 95% confidence level limits for the possible photon excess and the calculated Z^0 branching ratio limits for anomalous three body Z^0 decays are only given for the data at the Z^0 peak.

M_X	$X \to \ell^+\ell^-$	$X \to e^+e^-$	$X \to \mu^+\mu^-$	$X \to \tau^+\tau^-$
65 GeV	5.2	5.3	2.5	2.9
70 GeV	12	9.2	4.7	3.5
75 GeV	2.7	2.5	2.5	2.9
83 GeV	23	11	7.1	11

Table 3: Obtained 95% confidence level limits on the branching ratios in units of 10^{-5} for Z^0 decays into a photon and X for different M_X and subsequent X decays into a pair of charged leptons.

$\sqrt{s'}(GeV)$	40–60	60–70	70–78	78–84	$<\sqrt{s'}>=75$
$N^{measured}_{events}$	2	0	2	3	5
$N^{expected}_{events}$	0.9	1.6	2.7	3.8	8
$\sigma^{expected}_{Born}$ (pb)	36	23	23	36	24
$\sigma^{measured}$ (pb)	$80\pm^{76}_{36}$	< 43 (95% c.l.)	$17\pm^{16}_{8}$	$28\pm^{21}_{11}$	$15\pm^{8}_{6}$

Table 4: Observed and expected number of acollinear $\mu^+\mu^-$ events for the different effective dilepton centre-of-mass energies $\sqrt{s'}$ and the corresponding cross sections.

Figure Captions

FIGURE 1a-d: Scatter plots of $x_{Ecal} = E_{cal}/E_{cm}$ versus $x_{vis} = E_{vis}/E_{cm}$ of the accepted events; (a) all events and (b-d) events with zero, one and two muons. The lines indicate the cuts used to separate $\tau^+\tau^-(\gamma)$ events.

FIGURE 2: The collinear photon yield in $\mu^+\mu^-(\gamma)$ events as a function x_γ. The curve is a smooth representation of the expectations from the KORALZ Monte Carlo for $\mu^+\mu^-(\gamma)$ events with about a factor of four higher statistics than the data. The data entries have been corrected for background and efficiency.

FIGURE 3: The angular distribution of isolated photons with respect to the closest lepton for $e^+e^-(\gamma)$, $\mu^+\mu^-(\gamma)$ and $\tau^+\tau^-(\gamma)$ events for the different photon energies considered. The curves are smooth representations of the predictions from the KORALZ Monte Carlo. The distributions are shown for (a) x_γ between 0.02 and 0.1, (b) x_γ between 0.1 and 0.3 and (c) x_γ larger than 0.3. In (d), the x_γ spectrum is shown for isolated photons in the different types of $\ell^+\ell^-\gamma$ events.

FIGURE 4a-d: The obtained branching ratio limits at 95% confidence level of the $Z^0 \rightarrow X\gamma$ with subsequent decays of X into $e^+e^-(\gamma)$, $\mu^+\mu^-(\gamma)$, $\tau^+\tau^-(\gamma)$ and any type of charged lepton pair $\ell^+\ell^-$.

FIGURE 5a-b: The total scaled event energy (including the calculated photon energy) for acollinear $\mu^+\mu^-(\gamma)$ events is shown in (a). In (b) the measured cross sections for e^+e^- annihilation into $\mu^+\mu^-(\gamma)$ events are shown from TRISTAN to LEP energies including our result from the five events with an effective centre-of-mass energy between 60 GeV and 84 GeV with an average energy of 75 GeV.

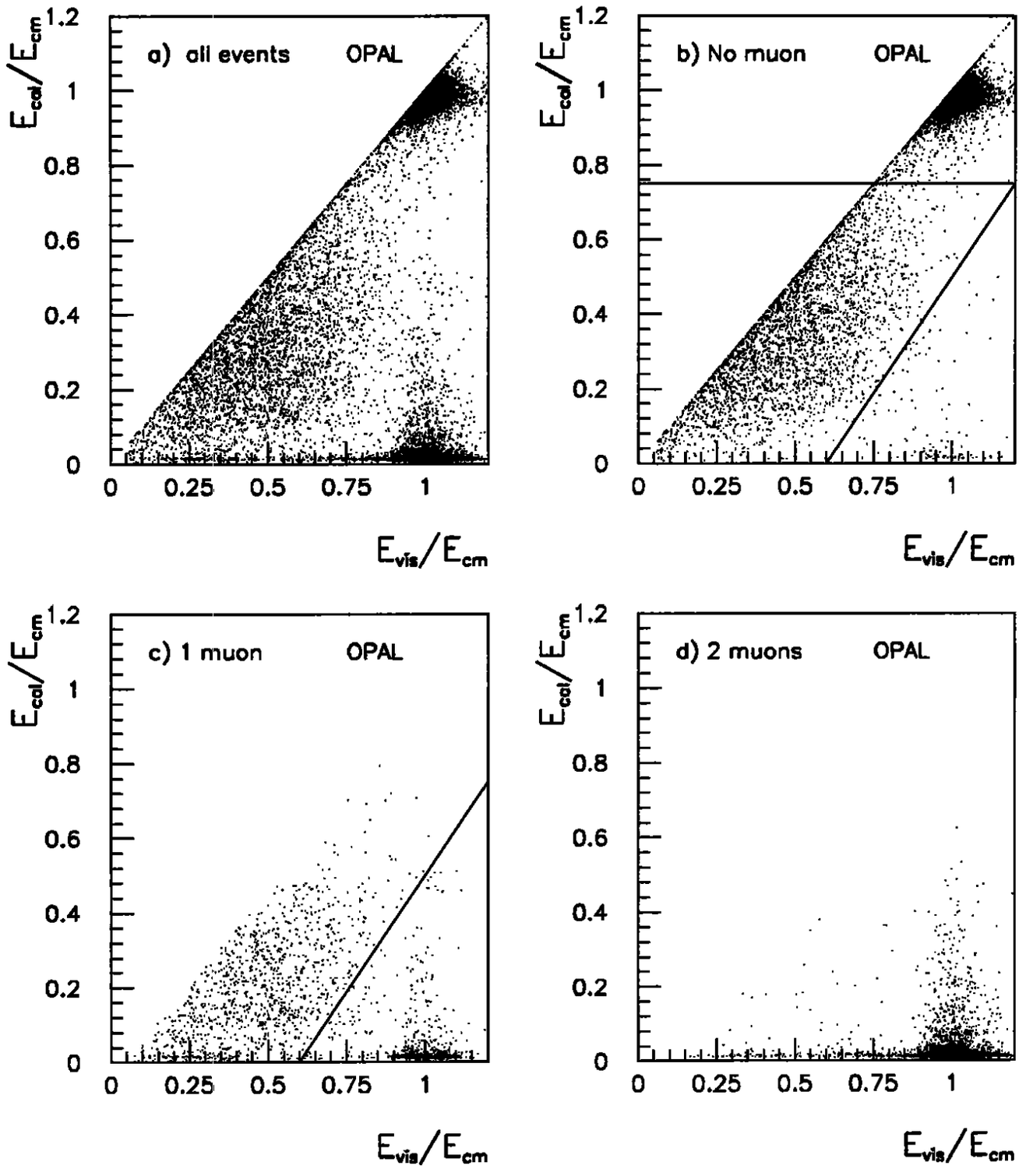
a) all events
OPAL
b) No muon
OPAL
c) 1 muon
OPAL
d) 2 muons
OPAL
E_{cal}/E_{cm}
E_{vis}/E_{cm}
0
0.2
0.4
0.6
0.8
1
1.2
0.25
0.5
0.75

Figure 1

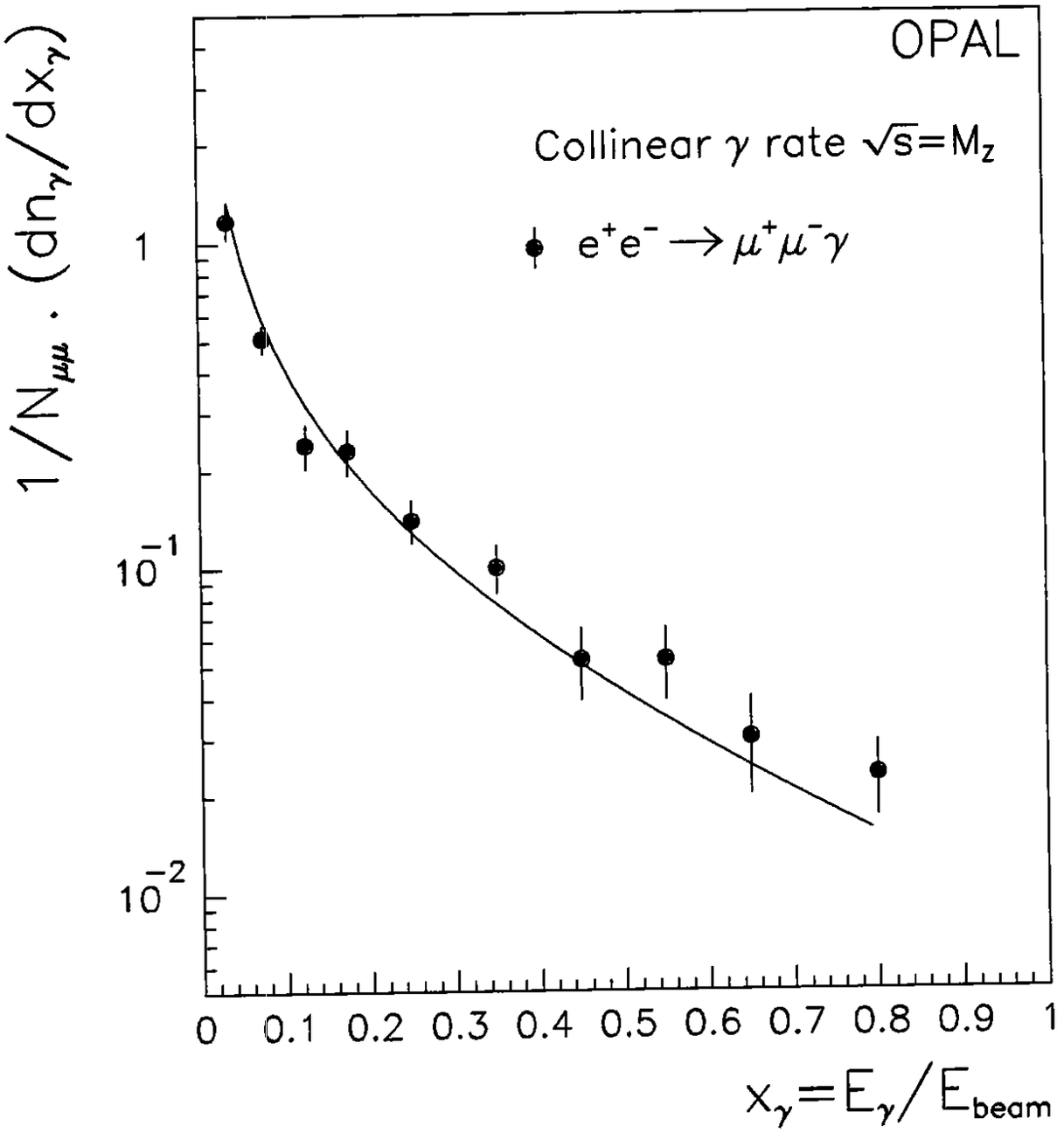
OPAL
Collinear γ rate √s=M_Z
e⁺e⁻ → μ⁺μ⁻γ
1/N_μμ · (dn_γ/dx_γ)
1
10⁻¹
10⁻²
0
0.1
0.2
0.3
0.4
0.5
0.6
0.7
0.8
0.9
1
x_γ = E_γ / E_beam

Figure 2

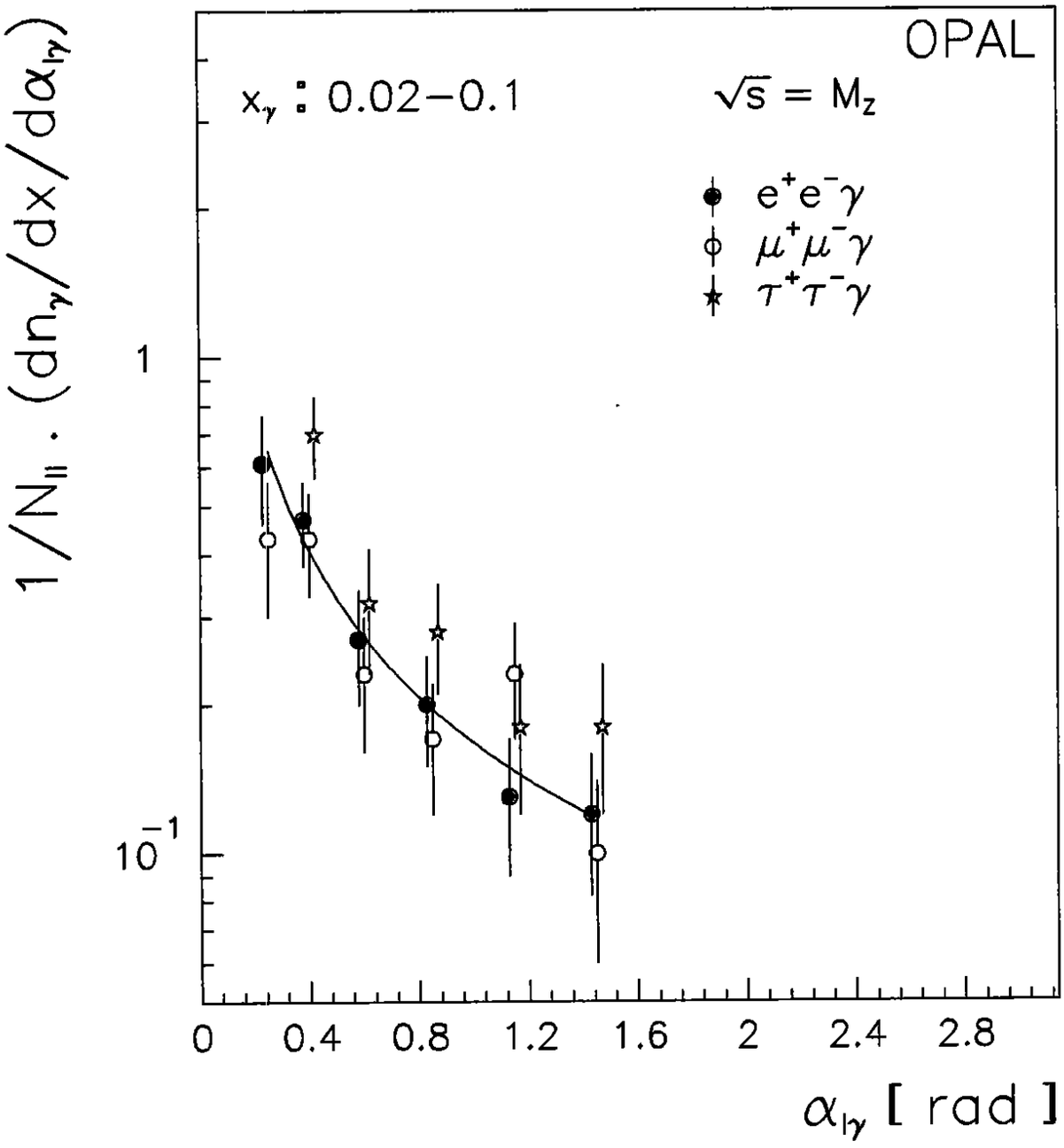
OPAL
x_γ : 0.02–0.1
$\sqrt{s} = M_Z$
$e^+e^-\gamma$
$\mu^+\mu^-\gamma$
$\tau^+\tau^-\gamma$
$1/N_{ll} \cdot (dn_\gamma/dx/d\alpha_{l\gamma})$
1
10^{-1}
0
0.4
0.8
1.2
1.6
2
2.4
2.8
$\alpha_{l\gamma}$ [rad]

Figure 3a

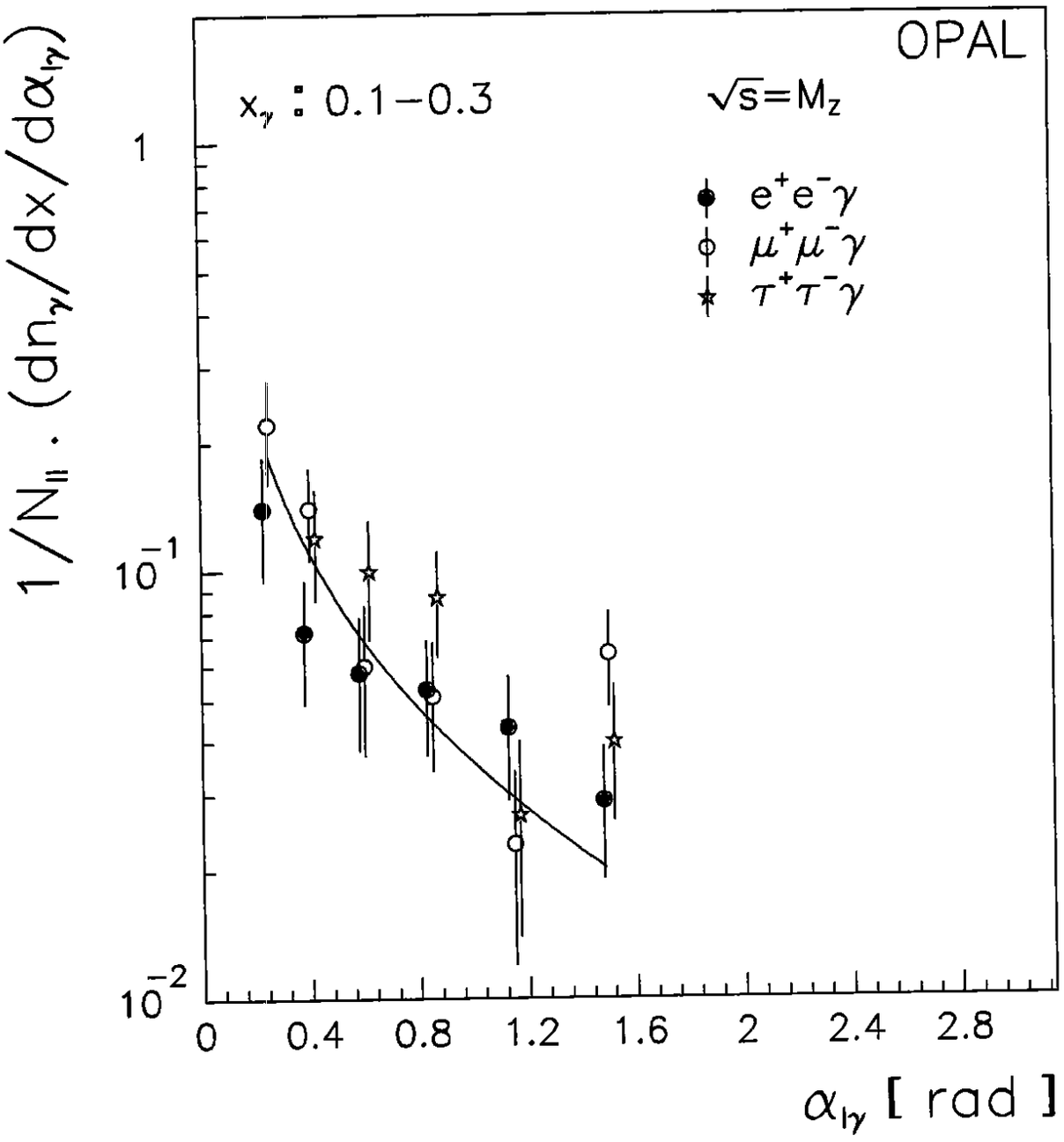
OPAL
x_γ : 0.1−0.3
$\sqrt{s}=M_Z$
$e^+e^-\gamma$
$\mu^+\mu^-\gamma$
$\tau^+\tau^-\gamma$
$1/N_{ll} \cdot (dn_\gamma/dx/d\alpha_{l\gamma})$
1
10^{-1}
10^{-2}
0
0.4
0.8
1.2
1.6
2
2.4
2.8
$\alpha_{l\gamma}$ [rad]

Figure 3b

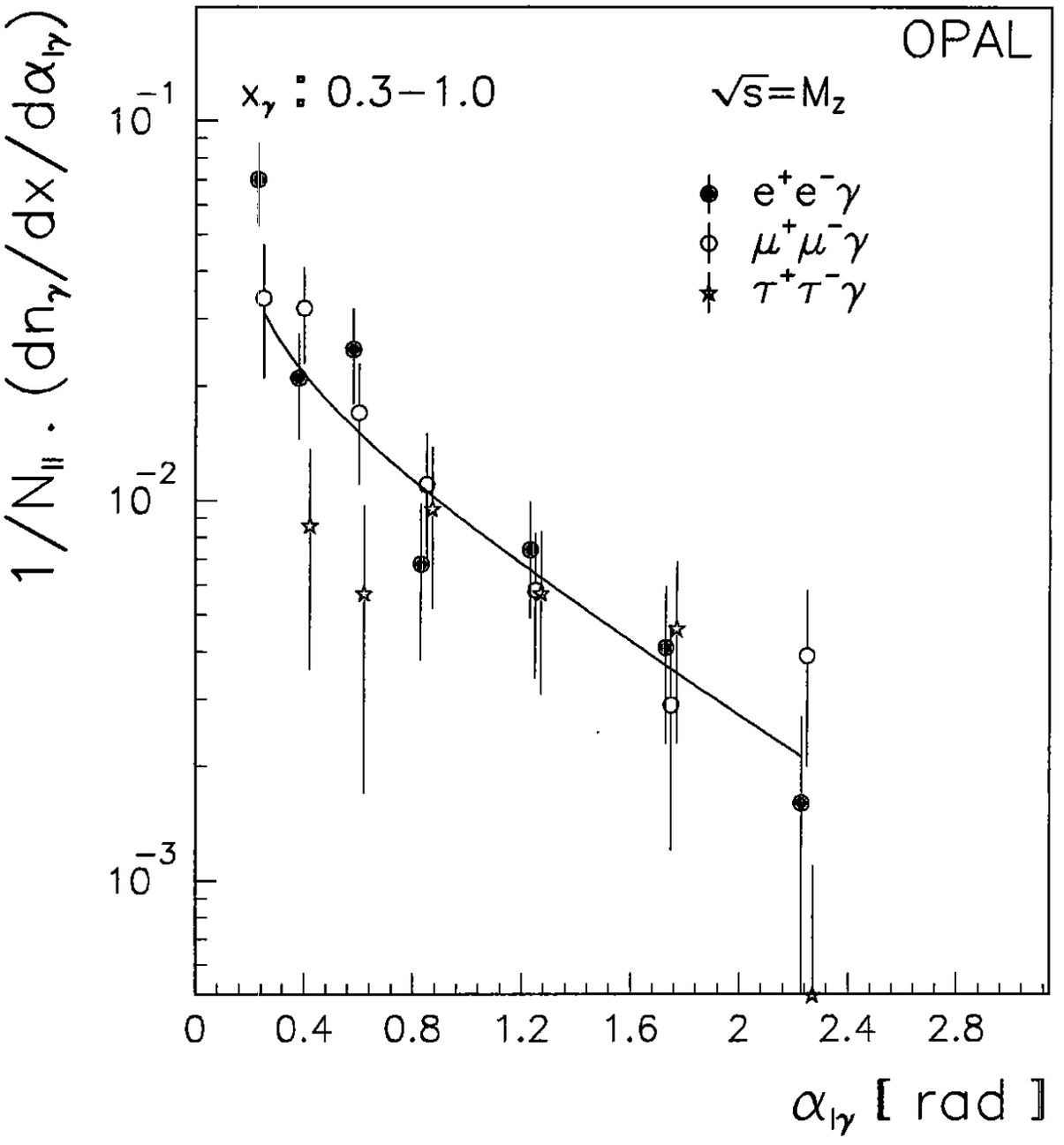
OPAL
x_γ : 0.3–1.0
$\sqrt{s}=M_Z$
$e^+e^-\gamma$
$\mu^+\mu^-\gamma$
$\tau^+\tau^-\gamma$
$1/N_{ll} \cdot (dn_\gamma/dx/d\alpha_{l\gamma})$
10^{-1}
10^{-2}
10^{-3}
0
0.4
0.8
1.2
1.6
2
2.4
2.8
$\alpha_{l\gamma}$ [rad]

Figure 3c

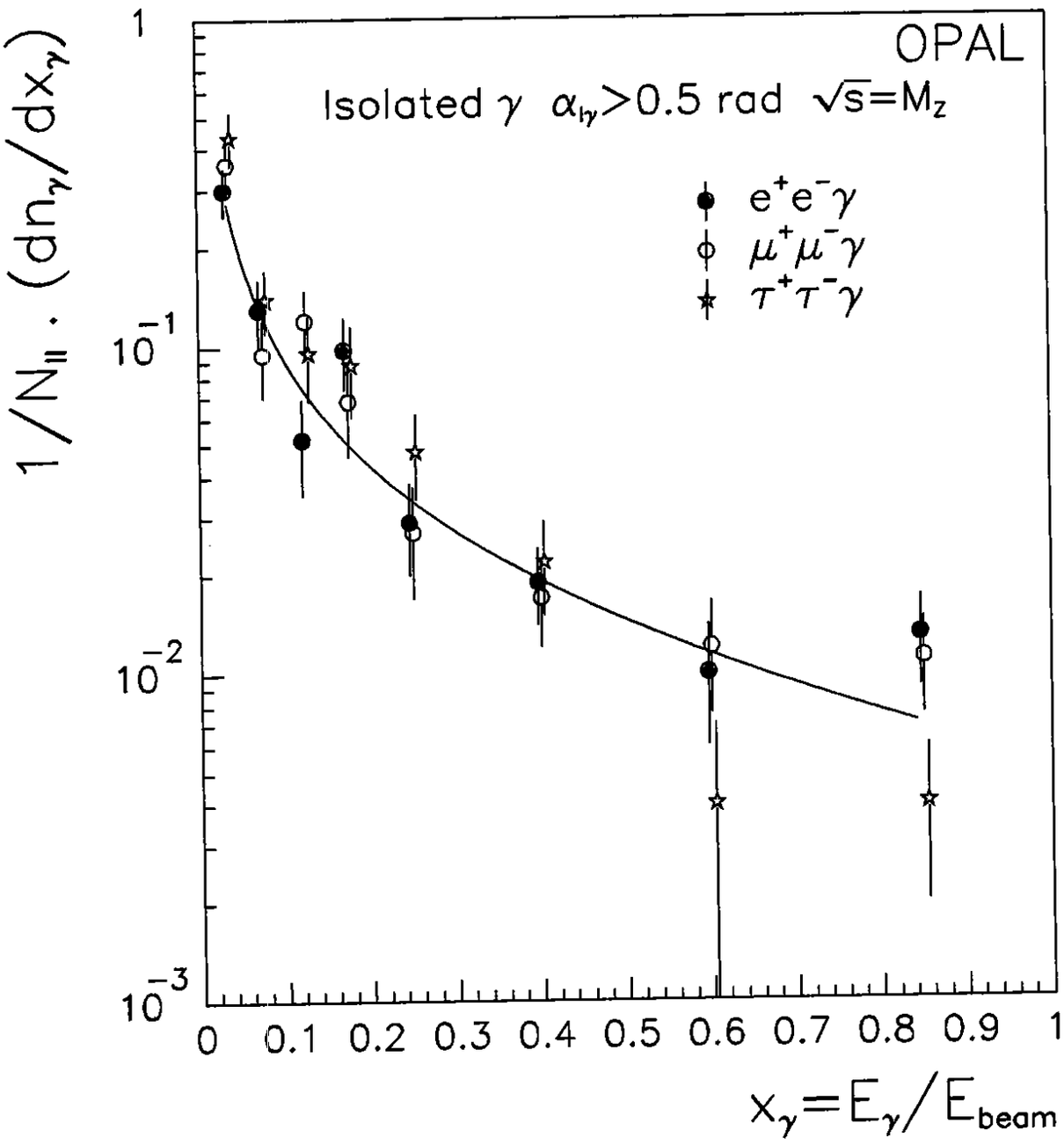
OPAL
Isolated γ $\alpha_{l\gamma}$>0.5 rad $\sqrt{s}=M_Z$
$e^+e^-\gamma$
$\mu^+\mu^-\gamma$
$\tau^+\tau^-\gamma$
$1/N_{ll} \cdot (dn_\gamma/dx_\gamma)$
1
10^{-1}
10^{-2}
10^{-3}
0
0.1
0.2
0.3
0.4
0.5
0.6
0.7
0.8
0.9
1
$x_\gamma = E_\gamma / E_{beam}$

Figure 3d

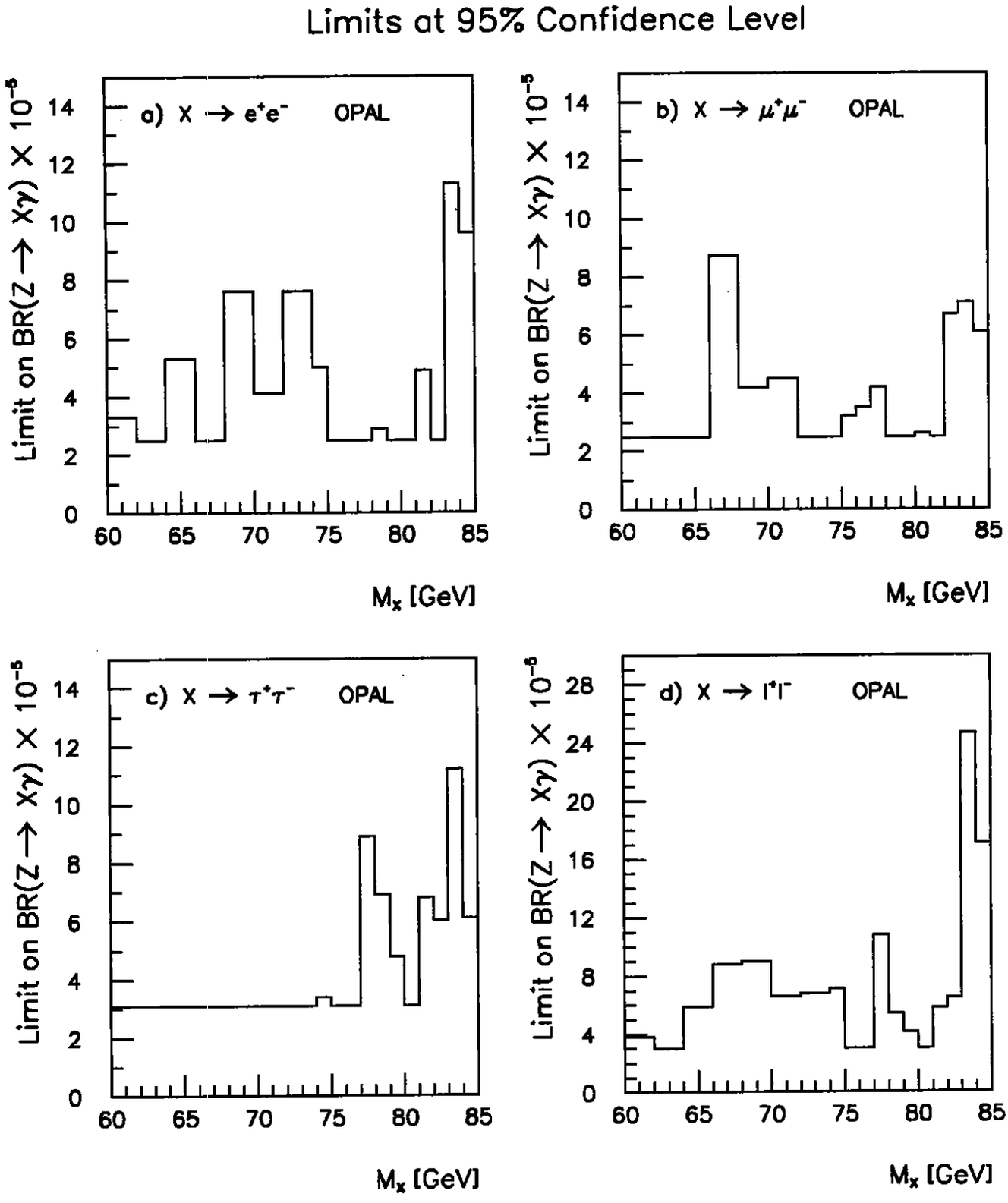
Limits at 95% Confidence Level
a) X → e⁺e⁻ OPAL
b) X → μ⁺μ⁻ OPAL
c) X → τ⁺τ⁻ OPAL
d) X → l⁺l⁻ OPAL
Limit on BR(Z → Xγ) X 10⁻⁵
M_X [GeV]

Figure 4

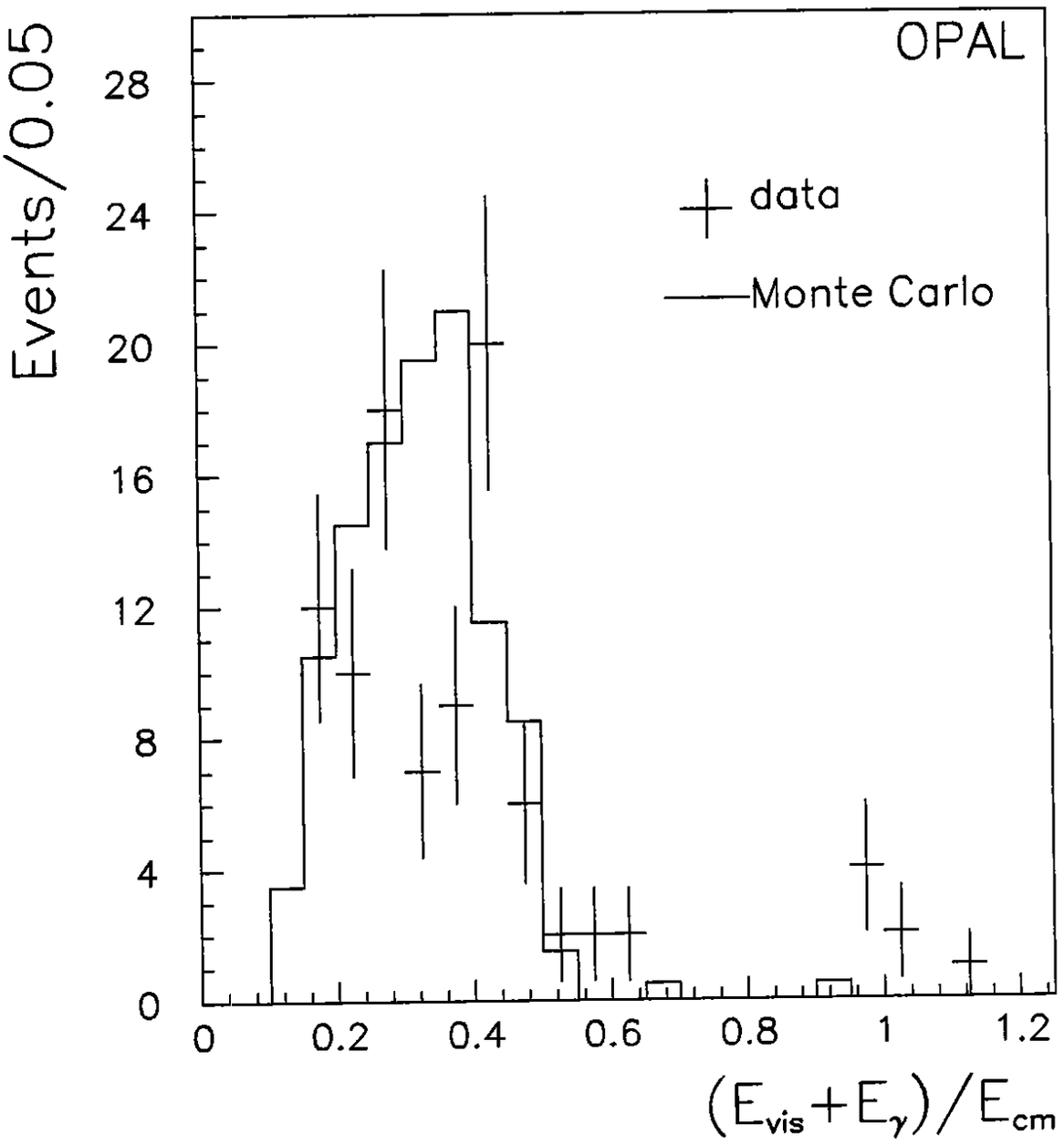
OPAL
data
Monte Carlo
Events/0.05
28
24
20
16
12
8
4
0
0
0.2
0.4
0.6
0.8
1
1.2
$(E_{vis}+E_\gamma)/E_{cm}$

Figure 5a

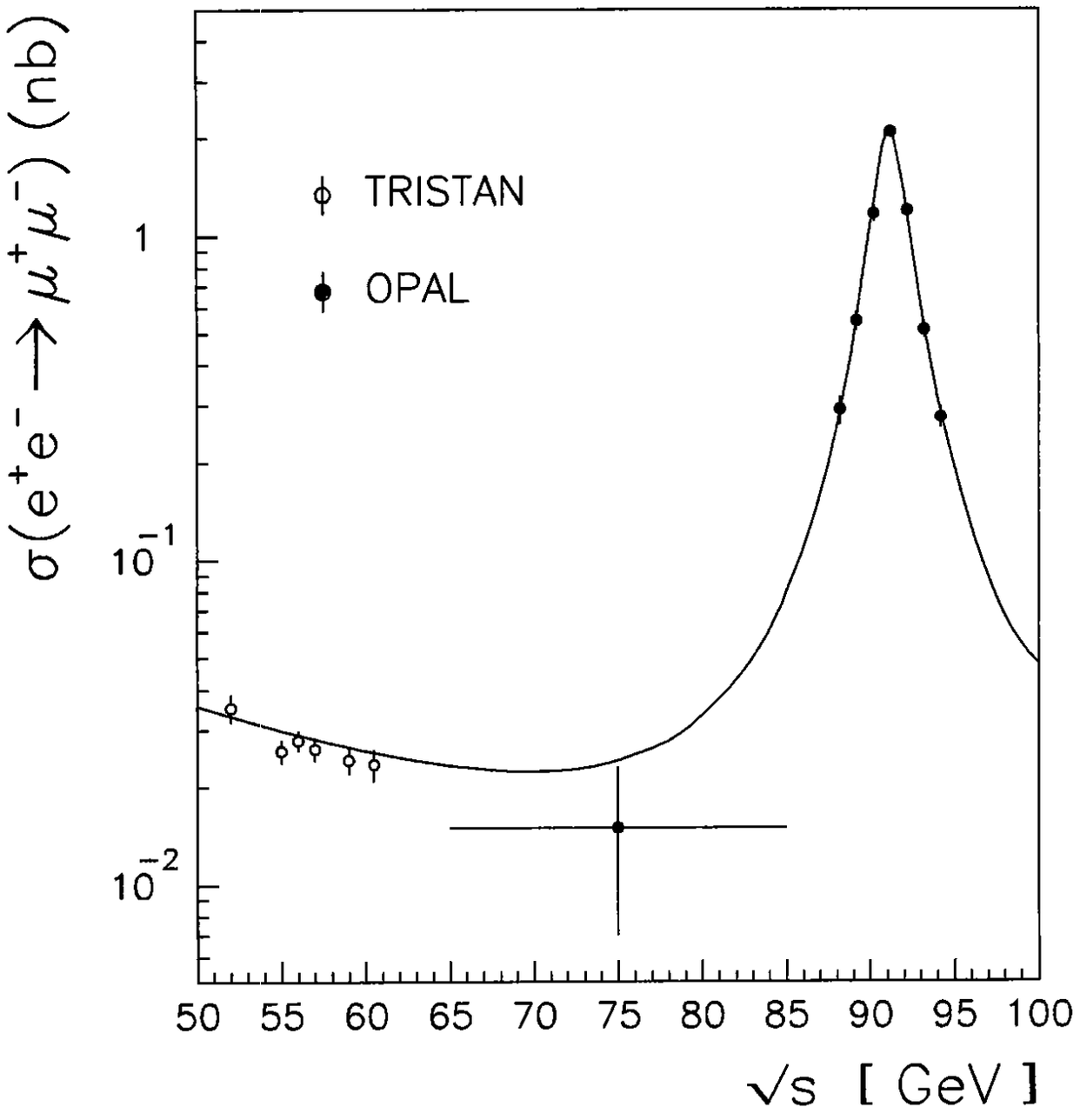
$\sigma(e^+e^- \rightarrow \mu^+\mu^-)$ (nb)
TRISTAN
OPAL
1
10^{-1}
10^{-2}
50 55 60 65 70 75 80 85 90 95 100
$\sqrt{s}$ [GeV]

Figure 5b